ELSEVIER

Available online at www.sciencedirect.com
SCIENCE DIRECT®

Microelectronic Engineering 77 (2005) 193–203

MICROELECTRONIC ENGINEERING

www.elsevier.com/locate/mee

Glycolic acid in hydrogen peroxide-based slurry for enhancing copper chemical mechanical polishing

Tzu-Hsuan Tsai [a,*], Yung-Fu Wu [b], Shi-Chern Yen [b]

[a] *Department of Chemical Engineering, Northern Taiwan Institute of Science and Technology, No. 2, Xueyuan Rd., Beitou, Taipei 112, Taiwan, R.O.C.*

[b] *Department of Chemical Engineering, National Taiwan University, Taipei 106, Taiwan*

Received 14 August 2004; accepted 30 October 2004
Available online 19 November 2004

Abstract

The effects of glycolic acid (GCA) added into hydrogen peroxide (H_2O_2) or urea-hydrogen peroxide (U-H_2O_2) slurries on Cu-CMP performance were investigated. Experiments showed that GCA could prevent H_2O_2 or U-H_2O_2 from rapid decomposition and increase the active peroxide lifetime of the slurries. In addition, electrochemical studies from polarization and impedance experiments verified that copper removal efficiency could be enhanced by use of GCA. Meanwhile, a valid equivalent circuit for Cu-CMP system was proposed, and the fitting results provided a good index to surface planarization. Furthermore, GCA could shorten the range of isoelectric points between Cu film and α-Al_2O_3 abrasives. After a post cleaning, the particle contamination thus could be reduced due to the electrostatic repulsion. Our study proved that adding GCA into the U-H_2O_2 slurries with BTA could further improve the Cu-CMP performance.
© 2004 Elsevier B.V. All rights reserved.

Keywords: Glycolic acid; Urea-hydrogen peroxide; Slurry; Copper; Chemical mechanical polishing

1. Introduction

Chemical mechanical polishing (CMP) of metal is widely recognized as the key technique to obtain global planarization for copper multilevel interconnection in IC manufacturing [1]. However, the planarization mechanisms of metal CMP involve complicated chemical reactions and physical actions. So it is difficult to control the CMP performance, especially for a high corrosion-sensitivity metal like Cu. According to different slurry components, the planarization mechanisms of metal CMP can be summarized as the following two types. The first one is that the metal surface may be polished with a dissolution-type slurry in which no surface film forms. In this case, the CMP

* Corresponding author. Tel.: +886228927154x8041; fax: +886228960255.
E-mail address: tzhtsai@ntu.edu.tw (T.-H. Tsai).

0167-9317/$ - see front matter © 2004 Elsevier B.V. All rights reserved.
doi:10.1016/j.mee.2004.10.008

process proceeds by the mechanical removal and chemical dissolution of metal itself [2]. In the second type of mechanisms, a thin abradable layer is continuously formed on metal surface by the reactions of metal and slurry components. These slurry components may include oxidants, inhibitors and other film-forming agents. The thin abradable layer is then scanned away rapidly by the mechanical action or dissolves in the slurry with a chelating agent. Once the mechanical polishing process has stopped, a thin passive film remains on the surface and inhibits the proceeding of wet etching [3]. Therefore, controlling CMP process to reach global planarization is much easier due to this mechanism.

The chemical components and properties of slurry determine the Cu-CMP performance principally. As a result, many studies devoted to the development of copper slurries with high planarization ability and CMP efficiency. According to the second mechanism mentioned above, oxidants with high oxidizing ability and low contamination should be required to form a passive film on Cu surface. Hydrogen peroxide (H_2O_2) is a widely used example at present [4,5]. However, H_2O_2 decomposes to H_2O and O_2 easily, and this decomposition will result in the slurry transport issues, unstable CMP performance and short shelf lifetime. Recently, urea-hydrogen peroxide (U-H_2O_2) has been proposed as the oxidant for Cu-CMP slurries due to its less self-decomposition and better oxidizing performance during CMP [6].

Also, Kaufman and Kistler [7] reported that organic acids can be added into metal slurries to enhance CMP performance by acting as pH adjusters or chelating agents. On the other hand, many researchers have examined the further efficiency of organic acids, and it was found that the action of organic acids would depend on the different CMP conditions. For instance, in 1999, Hu et al. [8] indicated that citric acid can inhibit Cu corrosion in HNO_3 slurries, and Zhang et al. [9] found that citric acid can prevent the alumina-particle deposition on tungsten surface. Even though many organic acids, such as acetic acid [10], oxalic acid [11], ethylenediamine tetraacetic acid (EDTA) [12] and amino acid [13,14] have been extensively studied, glycolic acid (GCA) has never been used. As known, GCA is easy handling, water-soluble, biodegradable, non-volatile and can efficiently chelate the metal. Therefore, the objective of this paper is to investigate the effect of GCA added into U-H_2O_2 slurries on electrochemical behaviors of Cu CMP. In addition to the measurement of polarization curves, the electrochemical impedance spectroscopy (EIS) was also obtained, and the equivalent circuit of surface reactions during Cu CMP was proposed. Although the equivalent circuits of Al have been discussed [15], fewer studies examined that in Cu CMP. In this study, the specific role of GCA and the information of the equivalent circuit for CMP in U-H_2O_2-based slurries were explored. Our experiments proved that GCA could improve Cu-CMP efficiency, and the planarization mechanisms of Cu CMP could be described well by the electrochemical methods.

2. Experimental

Commercial pure Cu sheets with 0.3-mm thickness were used, and the dimension of each specimen was 1×1 cm^2 for electrochemical measuring. In addition, 3-in. wafers with an electroplated Cu film were polished to obtain removal rates and surface roughness. All specimens were degreased by the cathode electrochemical method at 6 V for 20 s, and then were cleaned in 3 wt% H_2SO_4 solution followed by deionized (DI) water rinsing. Afterward, the samples were dried in nitrogen gas and transferred to the electrochemical measuring equipment or polishing machine. The slurry was prepared by use of 50-nm alumina particles (α-Al_2O_3), and its solid concentration in the slurry was fixed at 5 wt% for all of the experiments. To investigate the effects of different chemical components on Cu CMP, we prepared the slurries by analytical grade reagents, including urea-hydrogen peroxide (U-H_2O_2), benzotriazole (BTA) and glycolic acid (GCA).

For the purpose to compare the stability of solutions, 5 wt% U-H_2O_2 and 1.8 wt% H_2O_2, with the equal level of peroxide in solutions, were periodically analyzed by titration with 1 wt% potassium permanganate solution to determine the peroxide activity. An acoustic spectrometer, model

DT-1200, was used to determine the zeta potentials of materials in different pH values adjusted by HNO_3 or NH_4OH. Dipping experiments were conducted to determine the particle contamination on Cu surface. For dipping experiments, 300-nm α-Al_2O_3 particles were used in slurries for SEM observation. After dipped in slurries for 30 s, Cu samples were rinsed gently with DI water prior to SEM study.

The electrochemical test-cell was composed of Cu working electrode, platinum counter electrode and Ag/AgCl reference electrode, with a Luggin probe. The downward pressure and the rotating speeds during abrasion were 5 psi and 100 rpm, respectively. The dc electrochemical experiments were conducted by use of a potentiostat of EG&G, model 273A, while the corrosion software of EG&G, model 352, was adopted for electrochemical calculations. The dc polarization curves with a voltage scan rate of 5 mV/s were selected to measure the corrosion current densities and potential. Meanwhile, the corrosion current density was converted to the corresponding corrosion rate (CR) in nm/min according to Faraday's law. In addition, EIS measuring was performed with an electrochemical interface system of Solartron, FRA 1260 and 1286, and a small amplitude perturbation of 10 mV in a sinusoidal wave was applied with the operated frequency, 10^5–10^{-2} Hz, to ensure the linearity for impedance analysis.

For polishing experiments, a Lapmaster LM-51 polisher, operated at 80 rpm/60 rpm of the platen/carrier rotating speeds, was used with the polishing pad of IC 1000/SUBA IV supplied by Rodel. Before CMP, the slurry had to be stirred in a mixer to maintain the slurry suspension for the test period. During CMP, the slurry was delivered to the gap between Cu and the pad with a flow rate of 100 ml/min. The removal rate (RR) was calculated from the weight loss of Cu sheets before and after 5-min polishing, and the results were obtained by the average of three tests. Before or after CMP, the surface morphology of specimens was characterized by an atomic force microscope (AFM), and the surface rms-roughness (R_q) was calculated by the software package.

3. Results and discussion

3.1. Durability of slurries

As mentioned above, the oxidant acts an important role of film-formation in CMP slurry. In this study, we chose two peroxides, H_2O_2 and U-H_2O_2, as the oxidants. Table 1 lists the active percentages of H_2O_2 and U-H_2O_2, relative to their initial values, and the pH values in various hydrogen peroxide-based solutions. The results indicated that the active peroxide percentage in 1.8 wt% H_2O_2 solution degraded at a faster rate than that in 5 wt% U-H_2O_2 solution, but their pH values were similar. Additionally, the degradation rates of the active peroxide percentage showed large

Table 1
Changes of active peroxide percentage (%) and pH value with time in various H_2O_2 or U-H_2O_2 slurries

	Time (h)	0	10	50	100	250	500
1.8 wt% H_2O_2	%	100.0	96.35	75.16	57.42	41.99	33.44
	pH	5.56	5.52	5.31	5.45	5.03	5.18
1.8 wt% H_2O_2 + 1 wt% NH_4OH	%	100.0	23.75	20.12	18.15	16.41	15.08
	pH	10.03	10.21	9.78	9.65	9.41	9.32
1.8 wt% H_2O_2 + 1 wt% GCA	%	100.0	96.01	83.24	71.31	64.02	57.88
	pH	1.98	2.03	2.07	2.13	2.02	2.21
5 wt% U-H_2O_2	%	100.0	98.52	93.02	91.04	89.75	87.48
	pH	5.87	5.65	5.89	5.76	5.81	5.92
5 wt% U-H_2O_2 + 1 wt% NH_4OH	%	100.0	76.12	52.43	48.21	35.02	31.80
	pH	10.62	10.58	10.64	10.47	10.32	10.20
5 wt% U-H_2O_2 + 1 wt% GCA	%	100.0	97.82	96.01	94.23	93.31	91.59
	pH	2.04	2.10	2.08	2.11	1.94	2.07

variations when the U-H_2O_2 or H_2O_2-based solutions were mixed with NH_4OH or GCA. In Cu-CMP slurry, NH_4OH has been a well-known chelating agent. However, it was found the active peroxide percentage of 5 wt% H_2O_2 solution with 1 wt% NH_4OH reduced to 23.75% of its initial value after only 10 h. Even though H_2O_2 was replaced by U-H_2O_2, the peroxide activity of 5 wt% U-H_2O_2 solution with 1 wt% NH_4OH also reduced to 31.8% after 500 h. On the contrary, the addition of GCA, another chelating agent for Cu, could enhance the durability of slurries. After 500 h, the active peroxide percentage still exhibited a high level, 91.59%, for the 5 wt% U-H_2O_2 solution with 1 wt% GCA. Also, the 5 wt% H_2O_2 solution with 1 wt% GCA had higher peroxide activity than that with NH_4OH. This showed that using GCA as a chelating agent instead of NH_4OH could form a stable solution with a longer shelf lifetime for hydrogen peroxide-based CMP slurry.

3.2. Polarization curves

The abrasion effect on the polarization curves of Cu in various slurries are shown in Fig. 1 and Fig. 2, and their corresponding corrosion parameters and Cu removal rates (RR) are all listed in Table 2. The first thing noticeable is the difference between polarization curves of Fig. 1, especially the corrosion potential drop after abrasion (ΔE_d). It is obvious that ΔE_d in 1 wt% GCA slurry was smaller than that in 5 wt% U-H_2O_2. As reported [16], the potential drop is attributed to the change on sample surface from the formation of passive film to its removal. Therefore, as shown in Fig. 1, the larger ΔE_d in 5 wt% U-H_2O_2 illustrated a faster formation and a quicker removal of the passive film on Cu surface. On the other hand, Cu in 1 wt% GCA with a higher anodic current density, relative to 5 wt% U-H_2O_2, exhibited a faster dissolution rate of Cu due to the chelating action between Cu surface and GCA. In further comparison with the corrosion parameters in Table 2, the corrosion potential and corrosion current density were both higher in 5 wt% U-H_2O_2 than those in 1 wt% GCA. This was attributed to the Cu with higher oxidation state and greater oxidizing rate in U-H_2O_2 solution. Thus, it could be shown again that U-H_2O_2 owned a strong oxidizing action for Cu, and the formed passive film could protect Cu from deeper corrosion.

When 5 wt% U-H_2O_2 was mixed with 1 wt% GCA, ΔE_d decreased drastically but the anodic current density of Cu increased as shown in

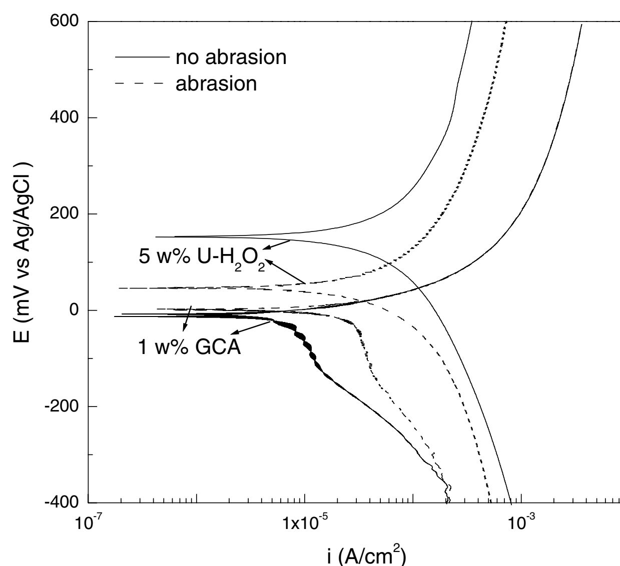

Fig. 1. Effect of abrasion on polarization curves for Cu in 5 wt% U-H_2O_2 or 1 wt% GCA slurry (abrasion: 5 psi and 100 rpm).

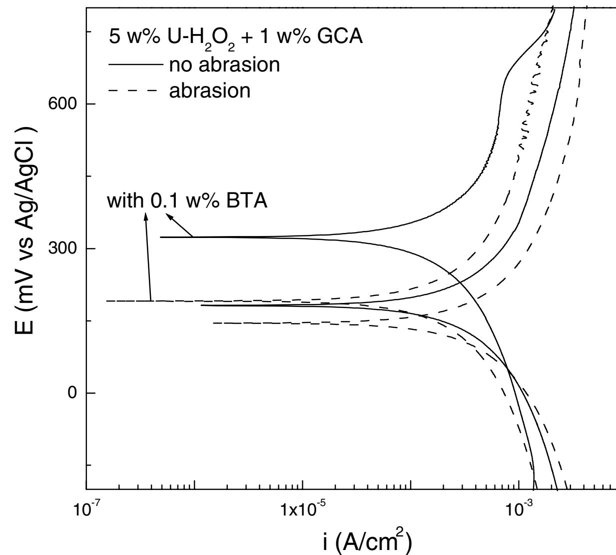

Fig. 2. Effects of abrasion and BTA on polarization curves for Cu in 5 wt% U-H_2O_2 with 1 wt% GCA slurries (abrasion: 5 psi and 100 rpm).

Table 2
Summary of corrosion parameters and removal rates (RR) of Cu in various slurries

Slurry	No abrasion		Abrasion		ΔE_d[a] (mV)	RR (nm/min)	CR (nm/min)
	E_{corr} (mV)	i_{corr} (A/cm^2)	E_{corr} (mV)	i_{corr} (A/cm^2)			
5 wt% U-H_2O_2	153	1.13×10^{-4}	46	1.33×10^{-4}	107	472.63	2.92
1 wt% GCA	−8	1.42×10^{-5}	3	4.48×10^{-5}	−11	184.30	1.07
5 wt% U-H_2O_2 + 1 wt% GCA	182	4.60×10^{-4}	145	8.85×10^{-4}	37	605.82	19.59
5 wt% U-H_2O_2 + 1 wt% GCA + 0.1 wt% BTA	323	9.63×10^{-5}	191	1.53×10^{-4}	132	594.14	3.37

[a] ΔE_d: $E_{corr(no\ abrasion)} - E_{corr(abrasion)}$.

Fig. 2. It resulted from the thinning passive film on Cu surface by the chelating action of GCA, so the Cu consumption was enhanced by both chelating and polishing. Thus, as listed in Table 2, the high corrosion rate, 19.59 nm/min, and removal rate, 605.82 nm/min, were obtained in the mixed slurry, 5 wt% U-H_2O_2 and 1 wt% GCA. Furthermore, Fig. 2 also shows that ΔE_d increased substantially by adding 0.1 wt% BTA into 5 wt% U-H_2O_2 and 1 wt% GCA slurry even though the current density still maintained a low level. It indicates that Cu in 5 wt% U-H_2O_2 slurry with 1 wt% GCA and 0.1 wt% BTA showed the high mechanical sensitivity and good anti-corrosion capability. As a result, the Cu removal rate attained 594.14 nm/min, but the corrosion rate reduced to 3.37 nm/min in this mixed slurry. The AFM micrographs of Cu surface before and after CMP with this slurry are shown in Fig. 3(a) and (b), respectively. In comparison with the AFM images, it shows the surface roughness could be reduced efficiently after CMP with the proposed slurry, 5 wt% U-H_2O_2, 1 wt% GCA and 0.1 wt% BTA.

3.3. EIS results

The EIS results of Cu in the slurry of 5 wt% U-H_2O_2, 1 wt% GCA and 0.1 wt% BTA are presented by Nyquist and Bode plots as shown in Fig. 4(a) and (b), respectively. When Cu was

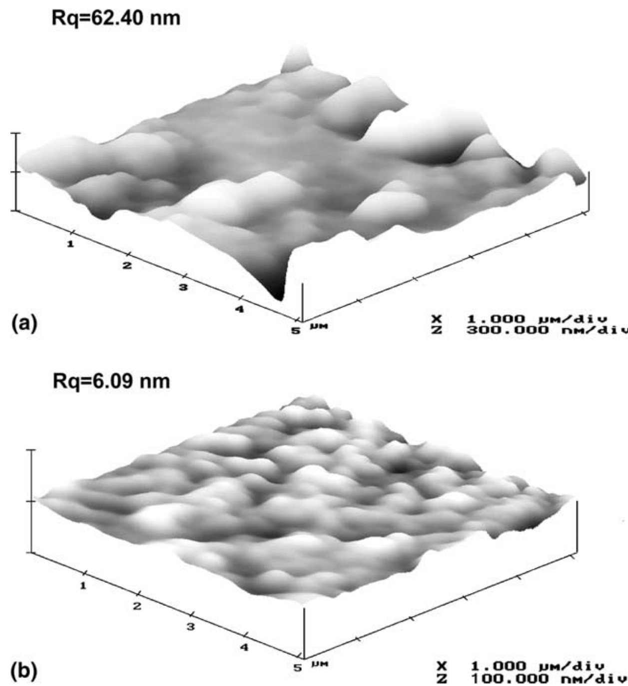

Fig. 3. AFM micrographs of Cu surface with roughness (R_q): (a) before CMP, and (b) after CMP with the mixed slurry, 5 wt% U-H_2O_2, 1 wt% GCA and 0.1 wt% BTA.

immersed in the mixed slurry, a dual non-ideal semicircle response of Nyquist plot, shown in Fig. 4(a), could be found. As Griffin et al. [17] pointed out, this response is caused from the formation of the secondary conduction paths or discontinuities within the copper oxide layer at or near the incoherent precipitates. Thus, the constant-phase-element (CPE) was adopted in the equivalent circuit to fit the behaviors at the interface of Cu and slurry [6]. Furthermore, it has been reported the inductor response in the low frequency range is due to the adsorption or the evolution of gas on surface [18]. Therefore, our equivalent circuit for describing Cu CMP would also contain the inductor element. In summary of the above facts, the electrochemical reactions at the interface of Cu and slurry would be simulated by the equivalent circuit of Fig. 5. As shown in this figure, the equivalent circuit consists of solution resistance (R_s), double-layer CPE (CPE_{dl}), charge-transfer resistance (R_{ct}), passive-film CPE (CPE_{pf}), passive-film resistance (R_{pf}) and adsorption inductance (L_{ad}). The fitting results by use of CPEs, presented by the solid lines in Fig. 4(a) and (b), would approach those experiment results rather than those by use of capacitors.

The results are also displayed by the Bode plot in Fig. 4(b). According to ac impedance theory [18], the impedance at frequency A and B, indicated by the dashed lines of Fig. 4(b), can be regarded as $R_s + R_{pf} + R_{ct}$, and $R_s + R_{pf}$, respectively, and the impedance at sufficiently high frequency, 10^5 Hz, is R_s. Thus, we could calculate these resistances from the Bode plot. It was found that R_s approached 78.88 $\Omega\,cm^2$ when Cu was immersed into the mixed slurry, 5 wt% U-H_2O_2, 1 wt% GCA and 0.1 wt% BTA. The polishing, however, increased R_s to 87.28 $\Omega\,cm^2$ due to the smaller fluid pathway between Cu surface and the pad. In addition, rise in R_{pf} and R_{ct} could be found with the increasing immersion time. The result indicated that the adsorbed BTA-layer and the formed oxide film inhibited the reactions continuously, and this caused the resistance to increase. As a

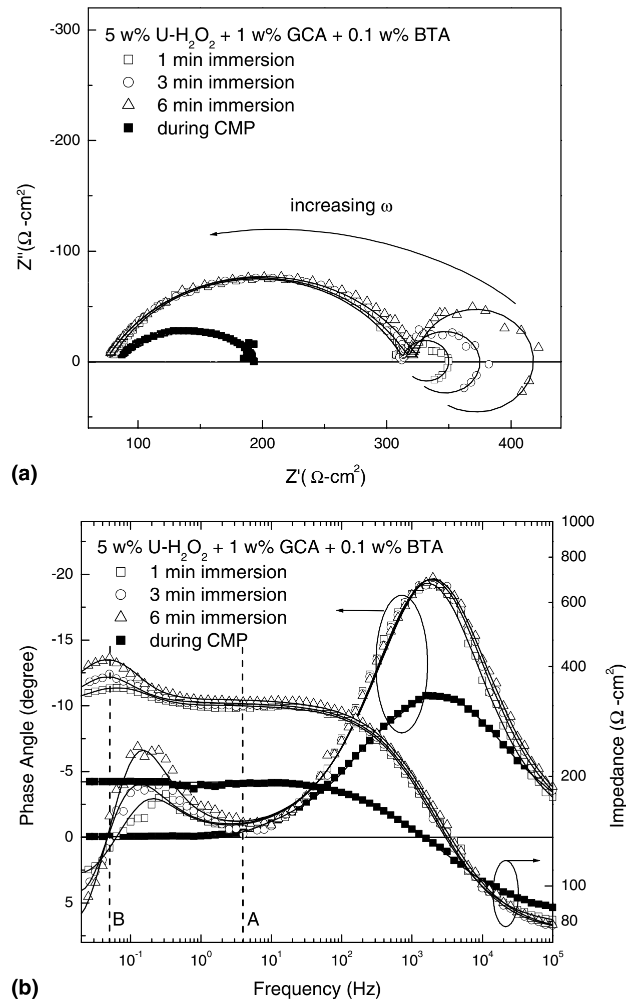

Fig. 4. Effects of immersion time and CMP on: (a) Nyquist plot and (b) Bode plot for Cu in 5 wt% U-H_2O_2, 1 wt% GCA and 0.1 wt% BTA slurry. Simulated results are represented by the solid curves (CMP: 5 psi and 100 rpm).

mechanical action of 5 psi and 100 rpm was applied, the adsorbed layers and passive films were destroyed, and then R_{pf} and R_{ct} reduced substantially.

Moreover, the phase angle in Fig. 4(b) also shows that the high-frequency peak was related to the passivation while the low-frequency peak was affected by the surface reactivity. The former was lowered in most of the CMP duration, and the latter was raised with the increasing immersion time. Also, the positive phase-angle value, depending on the adsorption, increased with the immersion time and disappeared during CMP. All of the above results indicated that the formation of gas, the adsorption of BTA-layer and the generation of oxide film on the Cu surface could be illustrated well by the proposed equivalent circuit, and also the behaviors sensitive to the mechanical force could be investigated.

3.4. Relationship between CPE and surface roughness

In our observations, the passive film on Cu surface was a loose oxide layer, and its surface was often rough and porous. So a non-ideal capacitor

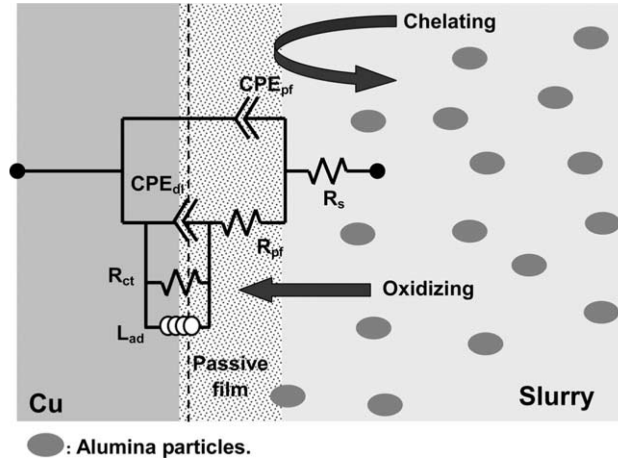

Fig. 5. Equivalent-circuit diagram and electrochemical characteristics used to fit the EIS results of Cu CMP as shown in Fig. 4.

was induced into the equivalent circuit for simulating the interface behaviors of Cu and slurry. The CPE herein was substituted for the ideal capacitor. The CPE impedance is written as [19],

$$Z_{\mathrm{CPE}} = [T(\mathrm{j}\omega)^n]^{-1},$$

where T is a general admittance function, j is the complex operator ($\sqrt{-1}$), and n is an adjustable parameter that usually lies between 0.5 and 1. When $n = 1$, the CPE describes an ideal capacitance with the high planarization or homogeneities. For the case of $n = 0.5$, a Warburg impedance relation is obtained; this impedance is associated with the concentration and the diffusion-related processes. Generally, the deviation from the ideal surface film, i.e. ideal capacitor, can be estimated by this adjustable parameter.

Fig. 6, containing the Cu-CMP results by use of U-H_2O_2-based slurries in Ref. [6], illustrates the dependence between the adjustable parameters and the roughness. In which, the parameters such as double-layer (n_{dl}) and passive film (n_{pf}) were included, and the roughness (R_q) was calculated by the AFM technique. Obviously, it exhibited that all of the n_{pf} values were lower than the n_{dl} values and independent of the roughness. On the contrary, n_{dl} seemed further relevant to the Cu surface roughness (R_q). The reason was evident that $\mathrm{CPE_{pf}}$ was involved in the porous passive layer while $\mathrm{CPE_{dl}}$ was affected only by the Cu surface. As a result, the n_{dl} value could provide a good index to monitor the planarization-performance on Cu surface. It was also found in Fig. 6 that the lowest surface roughness, 2.64 nm, was obtained in the U-H_2O_2 slurry mixed with 0.1 wt% BTA and 1 wt% NH_4OH instead of GCA. Even though the slurry containing GCA was not the best choice for planarity, the addition of GCA still could enhance the slurry stability. As reported [20], a stable slurry is important for good CMP performance because it can not only improve CMP reliability but also reduce the defects of the surface after CMP.

3.5. Surface potential and particle contamination

Fig. 7 shows the zeta potentials of Cu and α-Al_2O_3 particles as a function of pH in 0.1 wt% BTA solutions with or without 1 wt% GCA. The corresponding isoelectric points (IEPs), the pH of zero charge, of Cu and α-Al_2O_3 without GCA were 0.725 and 9.109, respectively. This meant that the Cu and α-Al_2O_3 surfaces had opposite charges for pH values from 0.725 to 9.109. The opposite charges resulted in the attraction, and then α-Al_2O_3 particles would be easily deposited on Cu surface and difficultly removed. However, when 1 wt% GCA was added to the solutions, the IEPs of Cu and α-Al_2O_3 reduced to 3.672 and 6.253, respectively. Obviously, the pH range of Cu and α-Al_2O_3 with opposite charges was shortened as shown in Fig. 7. This indicates that α-Al_2O_3 deposition could be inhibited by use of GCA due to the electrostatic

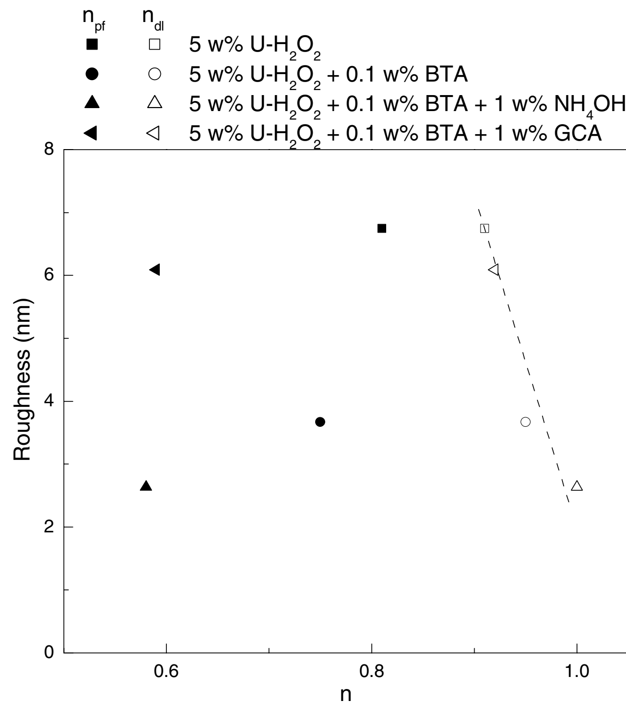

Fig. 6. Surface roughness vs. the adjusted parameters of passive film, n_{pf} (filled symbol) and double layer capacitances, n_{dl} (hollow symbol) in various slurries for Cu CMP at 5 psi and 100 rpm.

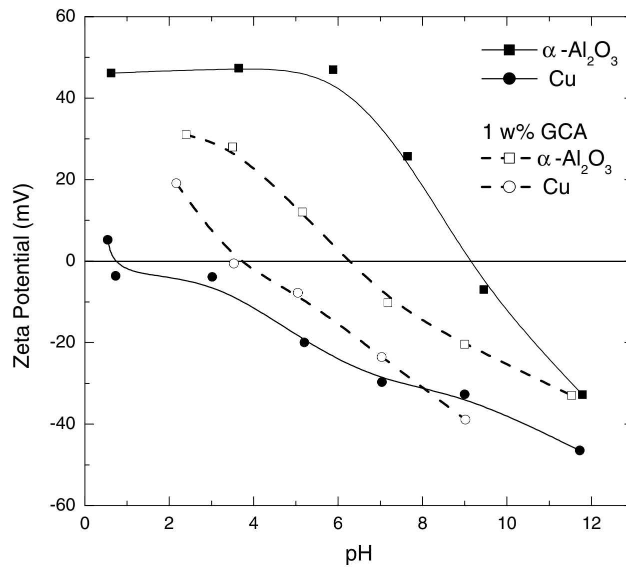

Fig. 7. Zeta potentials of α-Al_2O_3 and Cu as a function of pH in 0.1 wt% BTA solutions with or without 1 wt% GCA.

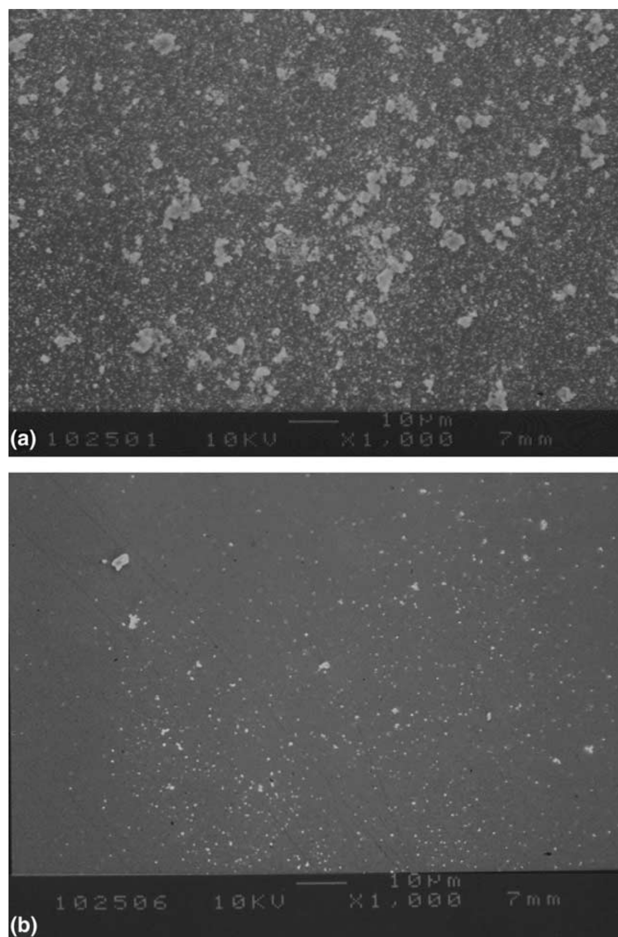

Fig. 8. SEM images of Cu samples dipped for 30 s in 5 wt% α-Al_2O_3 (300 nm) and 0.1 wt% BTA slurries: (a) without GCA; (b) with 1 wt% GCA.

repulsion. Fig. 8 displays the SEM images of α-Al_2O_3 contamination, shown by those white points, on Cu surface. It shows that a clearer Cu surface, with less α-Al_2O_3 deposition, was obtained by use of the slurry with 1 wt% GCA. These SEM images supported the above results of zeta potential.

4. Conclusions

In this study, the effect of glycolic acid (GCA) on Cu CMP was investigated by electrochemical methods, including titration, polarization and impedance experiments. The results showed that GCA could increase the stability of slurries by preventing the hydrogen-peroxide component from rapid decomposition. The electrochemical studies from polarization and impedance measurements verified that GCA could chelate with Cu and copper oxide on the polished surface in the existence of oxidants and inhibitors. Thus, the Cu-CMP performance could be enhanced by use of GCA, and the Cu removal rate could achieve 594.14 nm/min with a low surface roughness, 6.09 nm, in the mixed slurry, 5 wt% U-H_2O_2, 1 wt% GCA and 0.1 wt% BTA. In addition, a deliberate equivalent circuit for Cu-CMP system was proposed. The fitting results of EIS showed that the adjustable parameter of double-layer CPE (n_{dl}) would depend on the surface roughness and could be regarded as an index

to CMP planarization. The slurry with GCA still could result in the electrostatic repulsion between Cu surface and α-Al_2O_3 over a pH range larger than that without GCA. Therefore, the addition of GCA into copper slurries could efficiently decrease particle contamination and easily enhance the post-CMP cleaning process.

Acknowledgements

The authors would like to thank the National Science Council in Taiwan for financially supporting this research under Contract No. NSC 93-2214-E-149-001. Also, the authors are pleased to acknowledge the help extended by Northern Taiwan Institute of Science and Technology and National Taiwan University.

References

[1] H. Xiao, Introduction to Semiconductor Manufacturing Technology, Prentice-Hall, Inc., New Jersey, 2001.
[2] J.M. Steigerwald, R. Zirpoli, S.P. Murarka, D. Price, R.J. Gutmann, J. Electrochem. Soc. 141 (1994) 2842.
[3] F.B. Kaufman, D.B. Thompson, R.E. Broadie, M.A. Jaso, W.L. Guthrie, D.J. Pearson, M.B. Small, J. Electrochem. Soc. 138 (1991) 3460.
[4] M. Ziomek-Moroz, A. Miller, J. Hawk, K. Cadien, D.Y. Li, Wear 255 (2003) 869.
[5] T. Du, Y. Luo, V. Desai, Microelectron. Eng. 71 (2004) 90.
[6] T.H. Tsai, Y.F. Wu, S.C. Yen, Appl. Surf. Sci. 214 (2003) 120.
[7] V.B. Kaufman, R.C. Kistler, US Pat. 5,954,997, 1999.
[8] T.C. Hu, S.Y. Chiu, B.T. Dai, M.S. Tsai, I.C. Tung, M.S. Feng, Mater. Chem. Phys. 61 (1999) 169.
[9] L. Zhang, S. Raghavan, S. Meikle, G. Hudson, J. Electrochem. Soc. 146 (1999) 1442.
[10] J.M. Steigerwald, S.P. Murarka, R.J. Gutmann, D.J. Duquette, Mater. Chem. Phys. 41 (1995) 217.
[11] K. Yang, S. Avanzino, C.M.C. Woo, US Pat. 6,143,656, 2000.
[12] S. Aksu, F.M. Doyle, J. Electrochem. Soc. 149 (2002) B340.
[13] M. Hariharaputhiran, J. Zhang, S. Ramarajan, J.J. Keleher, Yuzhuo Li, S.V. Babu, J. Electrochem. Soc. 147 (2000) 3820.
[14] S. Aksu, F.M. Doyle, J. Electrochem. Soc. 149 (2002) B352.
[15] H.S. Kuo, W.T. Tsai, J. Electrochem. Soc. 147 (2000) 149.
[16] T.H. Tsai, S.C. Yen, Appl. Surf. Sci. 201 (2003) 190.
[17] A.J. Griffin, F.R. Brotzen, C.F. Dunn, J. Electrochem. Soc. 141 (1994) 3473.
[18] J.R. Macdonald, Impedance Spectroscopy, Wiley, New York, 1987.
[19] R. Babic, M.M. Hukovic, A. Jukic, J. Electrochem. Soc. 148 (2001) B146.
[20] L. Zhang, S. Raghavan, M. Weling, J. Vacuum, Soc. Technol. B 17 (1999) 2248.